
**Description of the Atmospheric Dispersion Model
ATSTEP**

Version RODOS PV 6.0 Final

RODOS migration
contract

D R A F T
V e r s i o n 2 . 0



RODOS
REPORT
DECISION SUPPORT FOR NUCLEAR EMERGENCIES

Description of the Atmospheric Dispersion Model ATSTEP - Version RODOS PV 6.0 Patch07
RODOS(RA2)-TN(04)-03

Jürgen Päsler-Sauer
Forschungszentrum Karlsruhe GmbH
Institut für Kern- und Energietechnik
Postfach 3640
D-76021 Karlsruhe
Email: juergen.paesler@rodos.fzk.de

Draft, 30 Juli 2007

Management Summary

This report describes the atmospheric dispersion and deposition model ATSTEP. The basic mathematical formulas used in the model are given and their physical meaning and model approximations are explained and illustrated. The use of additional models in ATSTEP for plume rise, deposition and depletion, daughter nuclide build-up, and gamma radiation is described. Furthermore the internal structure of the ATSTEP code and the use of the SUBROUTINE ATSTEP in RODOS diagnosis- and prognosis modules is shown. Subroutines used together with ATSTEP are described.

ATSTEP is a Gaussian puff model for distances up to 50 km. It was developed especially for quick simulation calculations in the case of accidental releases of airborne radioactive contaminants. In RODOS 6.0 the model can calculate real-time diagnoses of the radiological situation during or after a release without limitation of duration and interactive dispersion prognoses/episodes for up to 47 days. The radiological situation is described by the following results calculated with ATSTEP: the concentration in the air near ground (instantaneous and time-integrated), the contamination of ground surface (dry and wet), and the gamma radiation from ground and from the radioactive cloud. These results are presented as time dependent, nuclide specific fields in the whole calculation area in the environment of the source of the release. In ATSTEP the following phenomena are considered in the modelling of atmospheric dispersion and the radiological situation: time dependent meteorology (meteorological tower- or SODAR data, forecast data, inhomogeneous wind fields), time dependent nuclide-group specific release rates, thermal energy and rise of the puffs released, dry and wet deposition and corresponding depletion of the cloud, gamma radiation from cloud and from ground, radioactive decay and (in two special cases) build-up of daughter nuclides, and potential doses. ATSTEP's areas of application are accidental releases from nuclear installations, radioactive releases from transport accidents including fire, and from radiological dispersal devices (dirty bombs).

Different to classic puff models in ATSTEP no instantaneous puffs but time-integrated elongated puffs are released. The transport of each elongated puff is achieved by two trajectories attached to both ends of the puff. As these pairs of trajectories follow the inhomogeneous and variable 2D-wind fields step by step, also the elongated puffs perform all the necessary changes in position, shape, and orientation, like stretching, rotations, shrinking, and sideways drift.

Because of the large size of the elongated puffs the plume can be represented by a relatively small number of puffs. Correspondingly the number of time steps needed for the simulation of the release and the transport is small. The elongated puff approximation reduces the computing time of the model code, so that during less than 10 minutes real-time a complete dispersion and contamination prognosis can be performed with releases over several hours. Nevertheless the spatial and temporal resolution of the results is fully sufficient for the applications in the RODOS system.

The work described in this report has been performed with support of the European Commission under the contract "Migration of RODOS to practical applicability for supporting decisions in operational emergency response to nuclear accidents" contract RODOS Migration, contract no. FIKR-CT-2000-00077.

Table of Contents

1	Model description	7
1.1	Advection and Diffusion in ATSTEP	7
1.1.1	Time steps and puffs	7
1.1.2	puff trajectories	9
1.1.3	puff time-integral calculation with sideways drift of puffs	10
1.1.4	Transport in inhomogeneous, variable windfields	12
1.1.5	Dispersion parameters	12
1.1.6	Reflection at ground surface and lid on top of mixing layer	14
1.1.7	Vertical wind profile and concentration weighted transport velocity vector	14
1.1.8	Puff rise by thermal energy and initial momentum	15
1.1.9	Dirty Bomb and Transport Accidents	15
1.2	Deposition to surfaces and depletion of the cloud	17
1.2.1	Dry deposition: deposition velocities	17
1.2.2	Wet deposition: Washout	18
1.2.3	Deposition depending on location and puff depletion	19
1.3	Radioactive decay and build-up of daughter nuclides	20
1.4	Gamma radiation fields	21
1.4.1	Cloud gamma radiation	21
1.4.2	Ground gamma radiation	22
2	The ATSTEP-Code	23
2.1	ATSTEP in different RODOS ASY modules	23
2.1.1	ATSTEP in the prognosis module ALSMCprogn	23
2.1.2	ATSTEP in the interactive module QUICKPROGNO	23
2.1.3	ATSTEP in the diagnosis module Atstepdiagn	23
2.2	Inner structure of the ATSTEP code	24
2.3	Subsequent programmes of ATSTEP	26
3	References	29

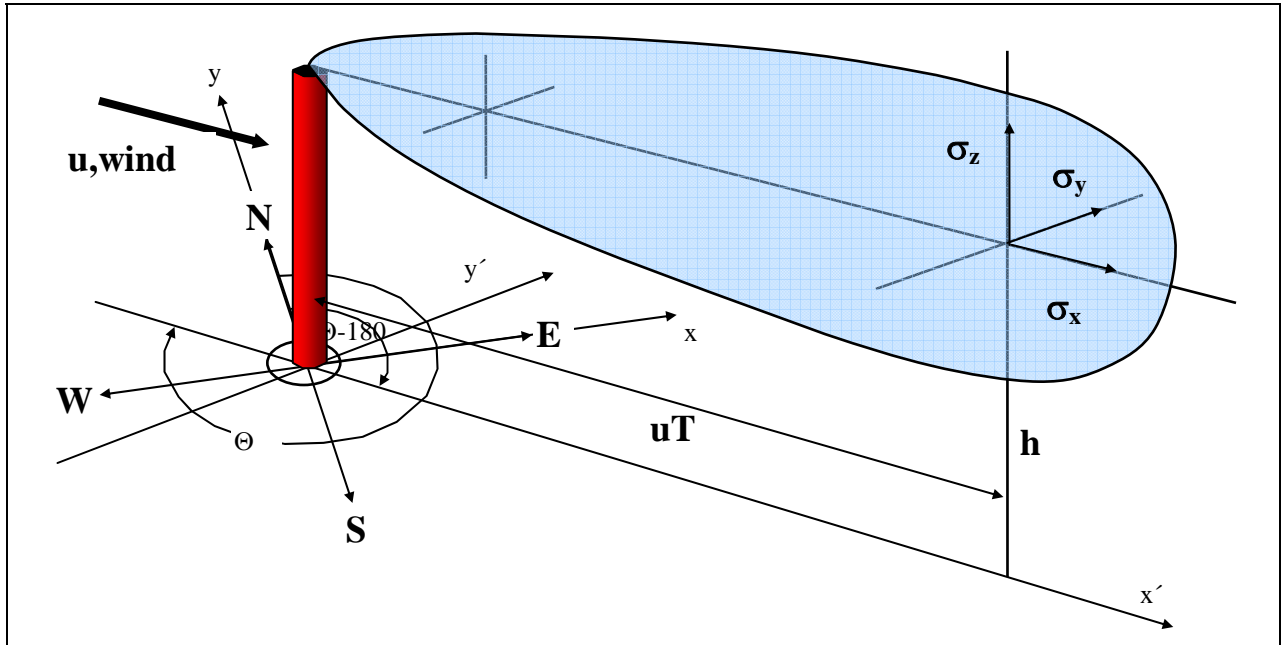
1 Model description

1.1 Advection and Diffusion in ATSTEP

1.1.1 Time steps and puffs

In ATSTEP the duration $T[s]$ of a release step equals the duration of the advection step. The release rate $QR[Bq/s]$ at the source and the wind velocity and direction $u[m/s]$ and $\theta[^\circ]$ are assumed to be constant during the time step. After each time step of duration T a puff is released from the source with a puff length $uT[m]$ and an puff axis direction $\theta-180^\circ$:

Fig. 1: Geometry for a puff release



The cross wind diffusion is modelled using horizontal and vertical Gaussian distributions normal to the puff axis; the corresponding sigma-parameters are σ_y and σ_z . They depend on the length coordinate x as in the Gaussian plume model. The longitudinal diffusion is modelled by error-functions with the parameter σ_x . Therefore the puff extends beyond the advection length uT (Fig. 2). The resulting concentration distribution of the puff equals the time-integral $TIC(x,y,z)[Bq.s/m^3]$ of a 3-dimensional Gaussian distribution χ_0 (ellipsoidal puff), that was advected from the source to the distance uT and that was extended corresponding to the increase of the σ -parameters (Eq. 1 and 2).

$$TIC(x, y, z) = \int_0^T \chi_0(x - ut, y, z - h) dt \quad (\text{Eq. 1})$$

$$\chi_0(x, y, z) = \frac{QR}{(\sqrt{2\pi})^3 \sigma_x \sigma_y \sigma_z} \exp\left(-\frac{1}{2}\left(\frac{x}{\sigma_x}\right)^2\right) \exp\left(-\frac{1}{2}\left(\frac{y}{\sigma_y}\right)^2\right) \exp\left(-\frac{1}{2}\left(\frac{z}{\sigma_z}\right)^2\right) \quad (\text{Eq. 2})$$

The computation of the time-integral TIC leads to the function $F(x)$, which is a superposition of error functions and models the length uT and the σ_x -diffusion of the puff..

$$\frac{1}{\sqrt{2\pi}\sigma_x} \int_0^T \exp\left(-\frac{1}{2}\left(\frac{x-ut}{\sigma_x}\right)^2\right) dt = \frac{1}{2u} \left(\text{erf}\left(\frac{x}{\sqrt{2}\sigma_x}\right) - \text{erf}\left(\frac{x-uT}{\sqrt{2}\sigma_x}\right) \right) =: \frac{F(x)}{u} \quad (\text{Eq. 3})$$

The complete concentration distribution of a puff (without ground surface and top of mixing layer reflection) is then given by:

$$\chi(x, y, z) = \frac{QR}{2\pi u \sigma_y \sigma_z} \cdot F(x) \cdot \exp\left(-\frac{1}{2}\left(\frac{y}{\sigma_y}\right)^2\right) \cdot \exp\left(-\frac{1}{2}\left(\frac{z-h}{\sigma_z}\right)^2\right) \quad (\text{Eq. 4})$$

A typical concentration distribution along the puff axis is shown in Fig. 2 a. The square with length uT corresponds to the puff's length without diffusion in x-direction, i.e. the plume segment's length. The slope of the curve in the middle of the picture results from the increasing dilution of the concentration due to the σ -parameters σ_y and σ_z . The tails of the curve result from the error-functions (Eq. 3) and represent physically the downwind and upwind diffusion along the puff axis. In this way the puff's concentration field is calculated from a plume segment's field by smearing it out along its axis in a mass conserving manner. Fig. 2 b shows the cross axis Gaussian distribution.

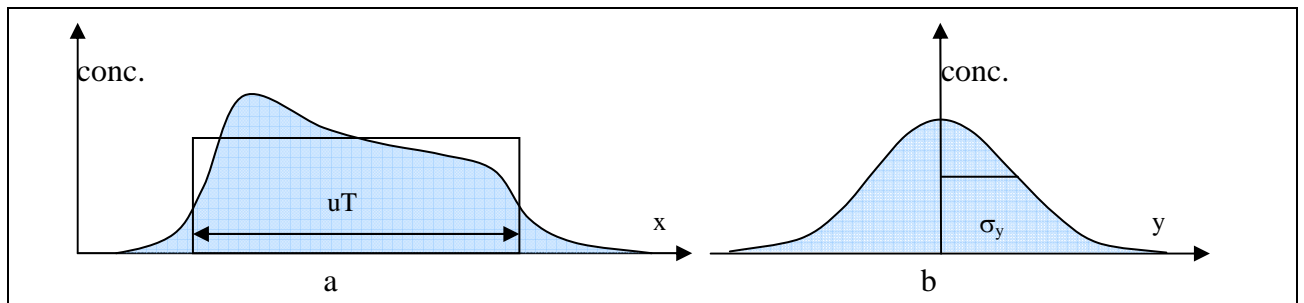


Fig. 2: Concentration curves on the puff axis and on the lateral y axis

1.1.2 puff trajectories

For determining the location, the orientation, and the spread of a puff during the transport in a variable wind field, **two trajectories are calculated for each puff**. They start at the source location and follow the movements of the start- and end-points of the puff axes in each time step during the atmospheric dispersion calculation. After each time step the change of orientation and length of the puff axis is determined corresponding to the local transport vectors $u_A(t)$ and $u_E(t)$ at the starting point A and the end point E of the puff i (see 2.1.7). The construction of the puff trajectories is carried out like shown in Fig.3 and results in $2n$ polygon curves in a plain layer at release height if n puffs were released. Because ATSTEP does not use 3-dimensional wind fields, but 2-dimensional wind fields plus vertical profiles, the trajectories are 2-dimensional curves in the height layer of the puff axis, except for the case of thermal puff rise (see 2.1.8).

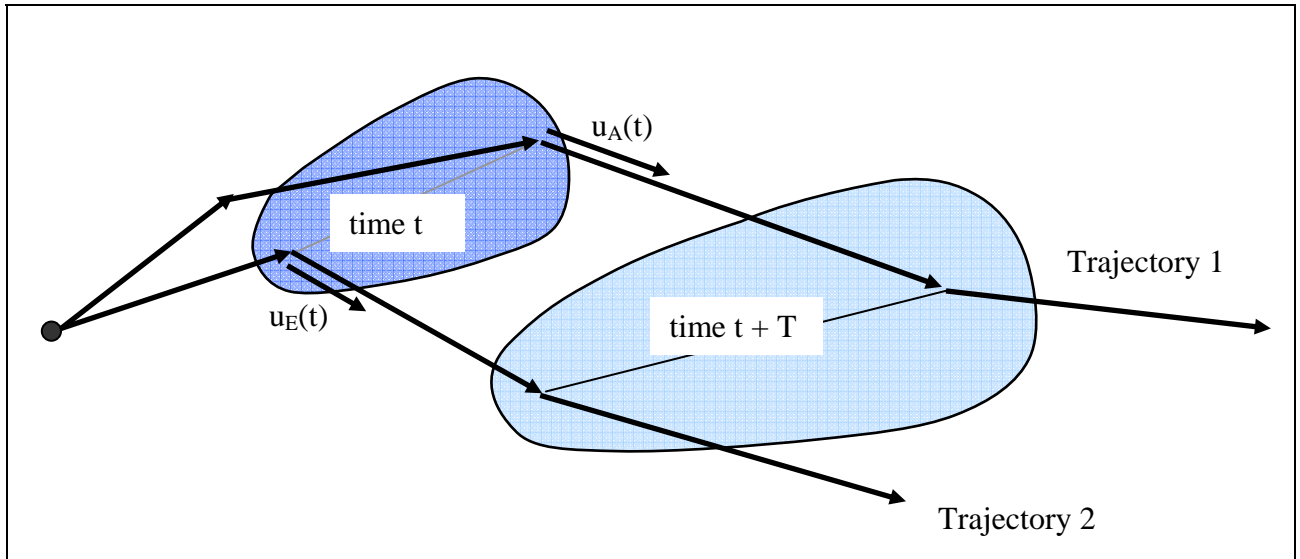


Fig. 3: Puff transport by a pair of trajectories

1.1.3 puff time-integral calculation with sideways drift of puffs

If wind fields depend on time generally the puff's transport direction will not be parallel to the puff's axis (sideways drift, Fig.3). Figure 4 shows the approximation that is used in ATSTEP to calculate time-integral of the air concentration if puff transport is sideways. The time-integral of the puff *i* during the step from *t* to *t+T* is shown by the grey shaded area. Because of the diffusion it is more extended than the area covered by the puff axis (the trapeze with wave pattern), and is mathematically described by a two-dimensional function $F(x,y)$ like in Eq. 3

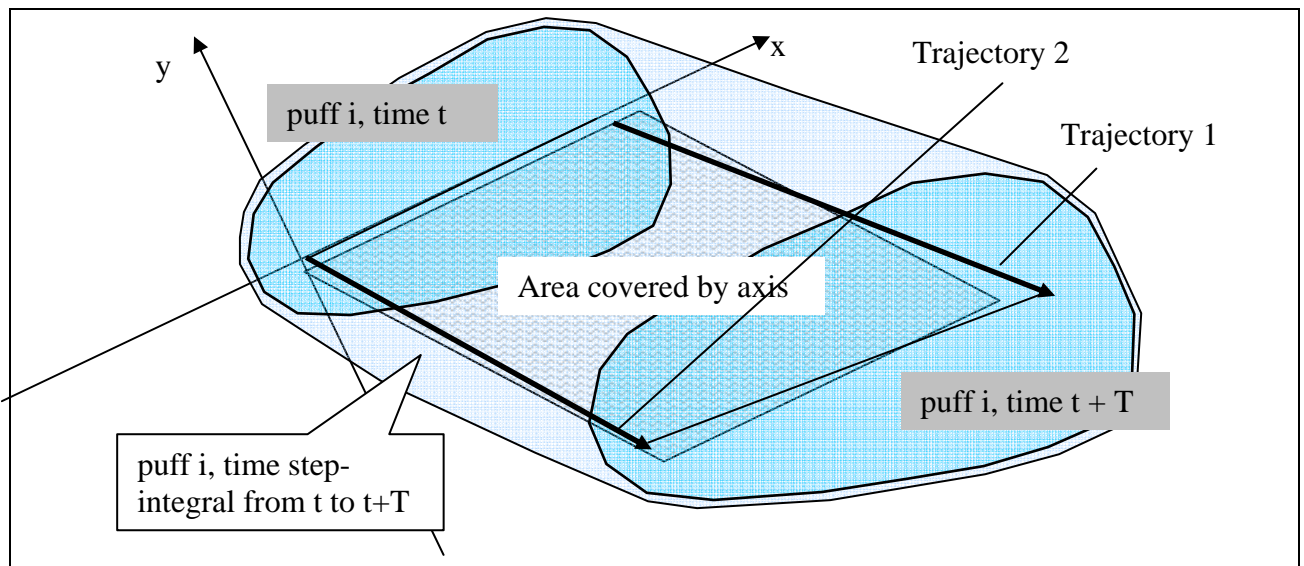
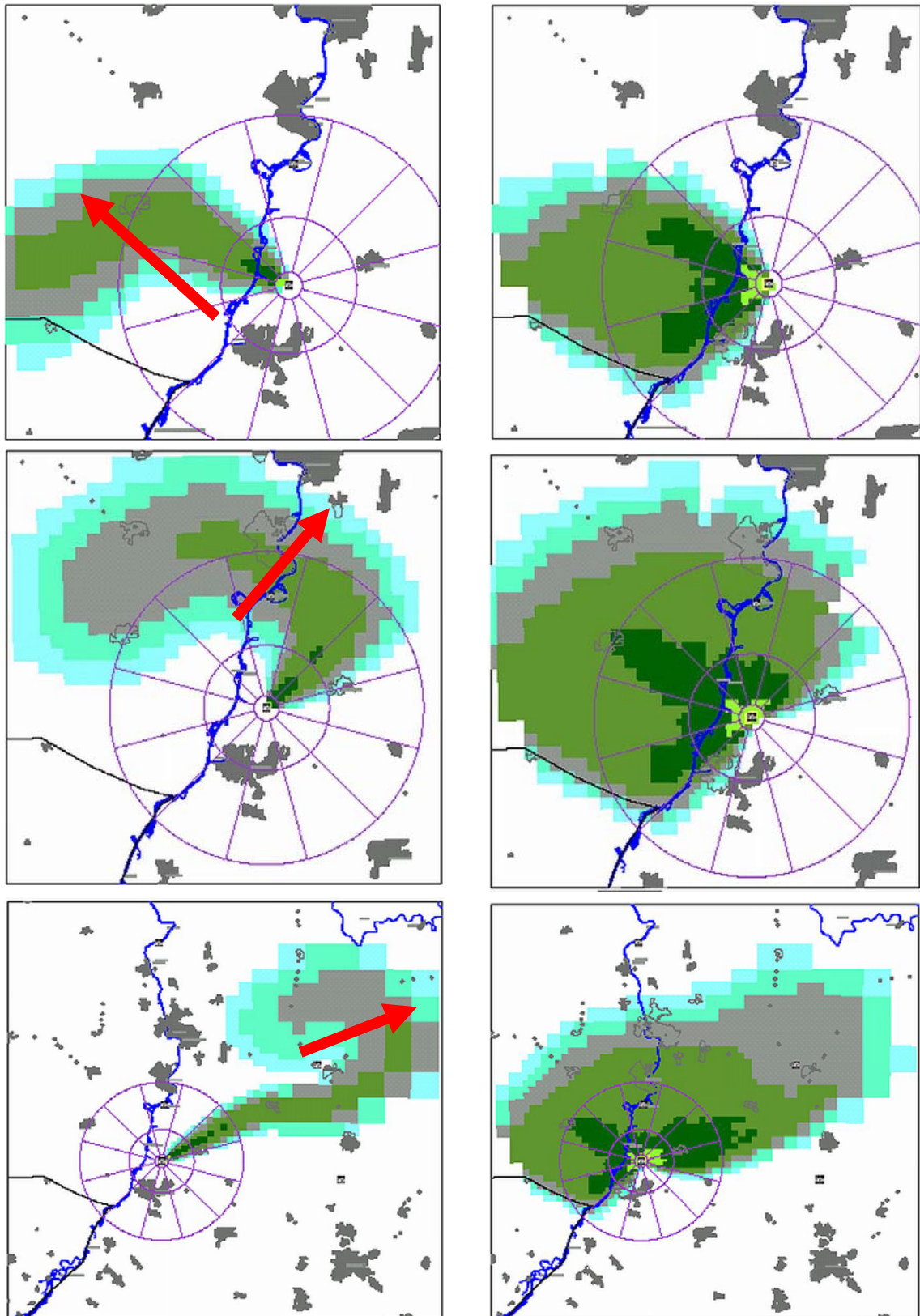


Fig. 4: Time-integral of a puff after one time step T



Calculated maps of near ground activity concentration in air of a spreading cloud from a continuous release of Kr 88. Variable wind and stability conditions. The outer circle has a radius of 25 km. The pictures in the left column show the instantaneous concentration in Bq/m³, the pictures in the right column show the corresponding time-integrated concentrations in Bq.s/m³, both at three different times after start of release. (Carried out with RODOS 6.0, QUICKPRO-ATSTEP).

1.1.4 Transport in inhomogeneous, variable windfields

The most general case is a spatially inhomogeneous, time dependent windfield. In this case the orientations and the lengths of the puffs change during the time step from t to $t+T$. The growth of the puffs by diffusion is taken into account by increasing the size of their σ -parameters corresponding to the increase of their total travelled distances.

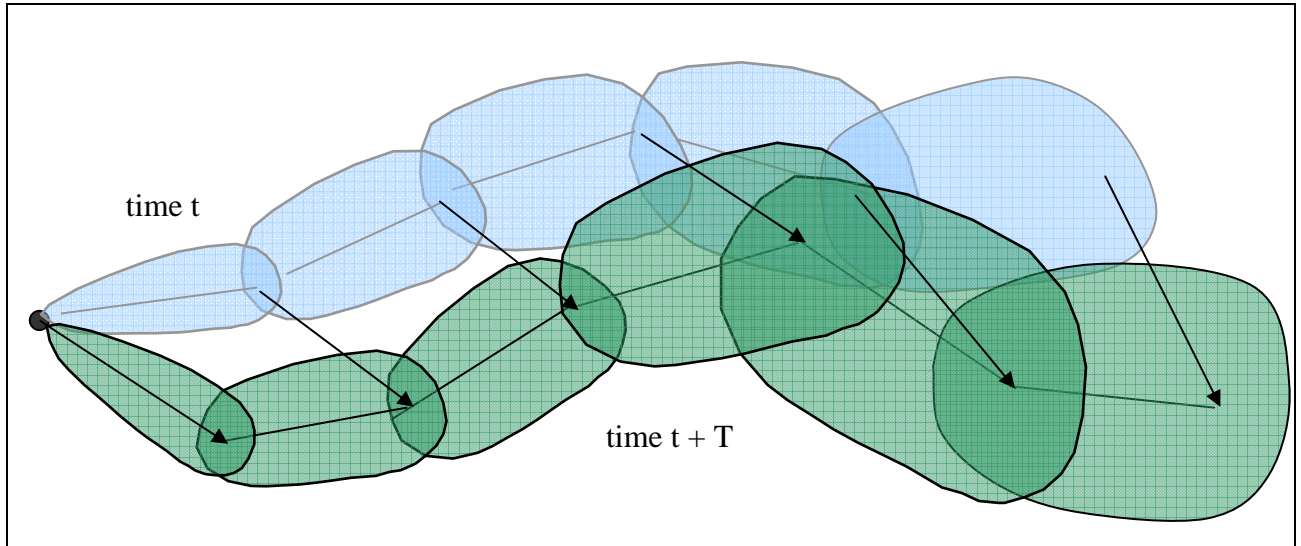


Fig. 5: Transport in inhomogeneous, variable windfield

1.1.5 Dispersion parameters

The modelling of turbulent diffusion in ATSTEP is parameterised by using diffusion parameters either depending on *travelled distance* (Eq. 5) or on *travelled time*(Eq. 6):

$$\sigma_y = p_y \cdot x^{q_y} \quad \sigma_z = p_z \cdot x^{q_z}, \quad \sigma_x \propto \sigma_\Theta \text{ oder } = \sigma_y \quad (\text{Eq.5})$$

$$\sigma_y = \sigma_y(t) \quad \sigma_z = \sigma_z(t) \quad (\text{Eq.6})$$

σ -parameters depending on *travelled distance*

In the case of dispersion parameters depending on *travelled distance* (Eq.5) there are 2 classes of roughness length ($z_0 = 0.5 - 1$ m and $z_0 = 1 - 1.5$ m). The dispersion parameters are defined by sets of dispersion coefficients p_y, q_y and p_z, q_z for σ_y and σ_z which are derived from tracer dispersion measurements. The **Mol-SCK-CEN parameters** set [1] corresponds to lower roughness length (rural, small houses, open or with trees), the **Karlsruhe-Jülich set**[2] corresponds to higher roughness (urban, with high buildings or forest). Both sets have 6 Pasquill-Gifford diffusion categories. The Karlsruhe-Jülich set is additionally defined for 3 different release heights: 50m, 100m und 180m.

The Karlsruhe-Jülich and Mol $\sigma_y(x)$ parameters generally are valid up to about $X_{valid}=10$ km of travelled distance. In case of the Karlsruhe-Jülich parameters, release heights above 75 m, and strong convective or very stable conditions (PG-categories A, B, or F), the corresponding X_{valid} is reduced to 2000, 4000, or 4000 m. Beyond X_{valid} the following $\sigma_y(x)$ parameterization is used in ATSTEP corresponding to Briggs[4]:

$$\sigma'_y(x \geq X_{valid}) = a \cdot \sqrt{x} \quad (\text{Eq.7})$$

Here a is defined such that $\sigma_y(x)$ changes smoothly into $\sigma'_y(x)$ at $x=X_{valid}$.

Diffusion along the axis of the puff is described by $\sigma_x(x)$. At small distances σ_x is determined from the horizontal wind direction fluctuation σ_θ corresponding to the dominating small scale turbulence. At larger distances σ_x is derived from σ_y .

The variable x used in this paragraph means the straight line way travelled like in the Gaussian plume model. Instead of this the trajectory lengths are taken in ATSTEP.

In ATSTEP all $\sigma(x)$ parameters are calculated by adding their differential increase during each time step, so that in each time step from t_1 to t_2 a change of the diffusion category is possible:

$$\sigma(x(t_2)) = \sigma(x(t_1)) + p \cdot (x(t_2)^q - x(t_1)^q) \quad (\text{Eq.8})$$

The σ -parameters $\sigma(x(t_2))$ at the trajectory point x at time t_2 are calculated from the parameters at the point $x(t_1)$ during the step from t_1 to t_2 , by adding the difference term in Eq. 8. The dispersion coefficients p and q are chosen corresponding to the actual diffusion category, puff height, and to the local roughness length defined by the land use. In case of variable land use under the flying puff therefore both Karlsruhe-Jülich and Mol parameters may contribute to its time-integrated plume.

Eq. 8 shows that growth of the $\sigma(x)$ parameters only can be achieved by a variation of x in time: ($x(t_2) \neq x(t_1)$). Therefore no turbulent broadening of the puffs would be possible during zero wind speed. In case of a local **zero wind speed** ATSTEP assumes a very small non-zero wind speed of 0.1 m/s and a zigzag-direction, causing the puff's head and/or end jitter to and fro a bit with the time steps. So the puff can grow though it is effectively not moving.

σ -parameters depending on *travelled time*

The time dependent dispersion parameters (Eq.6) are the sigma parameters σ_s of the spectral turbulence model which was chosen as a suitable common German-French model by the **German French Commission (GFC)** [3]. The variable t means the travelled time of each respective puff. Therefore a turbulent broadening of the puff is also possible during zero wind speed without change of puff location. The GFC- σ_s parameters continuously consider wind speed, height of the puffs, roughness length, Monin Obuchov length, and the friction velocity. The σ_s parameters are calculated outside ATSTEP with the new meteorological data during each time step and are stored in a table with travelling times of 0-10000 seconds. During the dispersion calculation step in ATSTEP the sigma parameter values $\sigma_{xyzE}(t)$ and $\sigma_{xyzA}(t)$ at both puff ends are taken from the table and interpolated corresponding to their travel times for all released puffs.

1.1.6 Reflection at ground surface and lid on top of mixing layer

In the Gaussian modelling of the vertical concentration profile total reflection of the concentration at the ground surface and the top of the mixing layer are assumed. The reflection at ground surface enhances the air concentration close to the surface by a factor of 2. The additional reflection at the top of the mixing layer causes the air contamination to get trapped in the mixing layer. Turbulent vertical mixing finally generates a uniform profile of the vertical contamination that is inversely proportional to the mixing height h_{mix} . In the model this is approximated by replacing $\sigma_z(x)$ by $\sim 0.8 \cdot h_{mix}$ in Eq. 5, if $\sigma_z(x)$ exceeds 80% of the mixing height (Eq. 8):

$$\sigma_z(x) \geq \sqrt{\frac{2}{\pi}} \cdot h_{mix} = 0.8 \cdot h_{mix} \quad (\text{Eq. 9})$$

$$\chi(x, y, 0) = \frac{Q}{\pi \sigma_y(x) \cdot 0.8 \cdot h_{mix} \cdot u} \cdot F(x) \cdot \exp\left(-\frac{1}{2} \left(\frac{y}{\sigma_y}\right)^2\right) \cdot (\text{Eq. 10})$$

In a Gaussian puff model material of a puff can not penetrate the inversion lid of the mixing layer. Neither can a puff that has expanded vertically to a given mixing layer height during day time shrink to smaller heights if the mixing height comes down during night time. The vertical extension of a puff can only stay constant or grow. Therefore in the model each puff gets it's own history of mixing heights which can stay constant (if the real mixing height falls), or increase to a higher real mixing height.

1.1.7 Vertical wind profile and concentration weighted transport velocity vector

Wind speed and direction generally depend on height. The wind speed profile is generated in the meteorological pre-processor in the form of a power law (Eq. 11) from wind data measured at various heights. The directional shear profile is assumed to change linearly with height below 200 m. If there is only one measurement height a default power law profile is used for defining the wind at other heights. In this case no directional shear with height is assumed. The power law profile parameter (wind profile exponent WP) depends on diffusion category and roughness length z_0 :

$$u(z) = u(z_m) \cdot \left(\frac{z}{z_m}\right)^{WP} \quad (\text{Eq. 11})$$

The resulting transport velocity vectors with which the head and the end of each puff are moved along their trajectories are *not just equal* to the wind vectors at puff axis height. This happens because of the concentration profiles *and* wind profiles involved: The bottom parts of a concentration cloud move more slowly and into another direction than the top parts. Nevertheless each puff has to be transported *as a whole* using two effective transport velocities at the head and the end of each puff. To determine the mass profile weighted transport velocity vectors the vertical profiles of concentration *and* of the wind vector are taken at 9 different levels of height. The weighted sum over these height levels then leads to the effective transport velocities.

1.1.8 Puff rise by thermal energy and initial momentum

If thermal energy or initial vertical momentum is released with a puff the rising phase and the final rise is considered in the form of a rising trajectory of this puff.

In the rise model first the relations of volume flux, exhaust velocity and temperature contained in the release data are transformed into a criterion for buoyancy or momentum dominated rise. Then the rise phase of either a thermal or a momentum release is calculated taking into account neutral, stable, and unstable atmospheric stratification, and the corresponding wind profile following the plume rise model of Briggs [5].

From this the final rise of the puff Δh_{fin} and the corresponding distance x_{fin} is derived. The rising phase of the puff trajectory is then calculated as a $x^{2/3}$ -curve like in Fig. 6. The model does not allow for puffs penetrating the lid of the mixing layer.

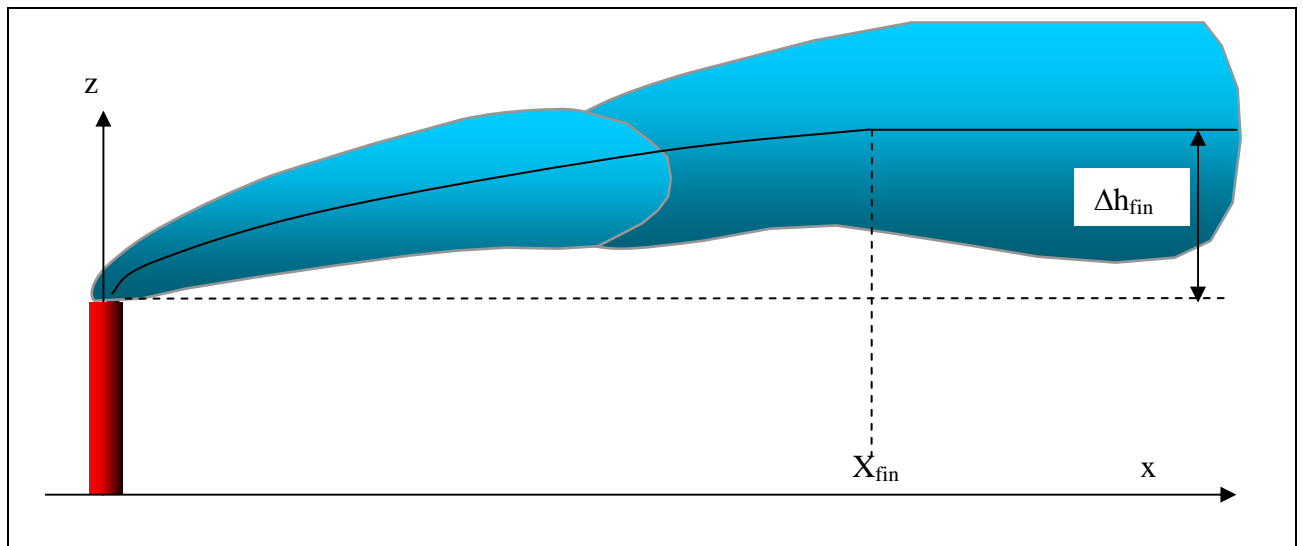


Fig. 6: Trajectory of a puff with rise by thermal energy or initial vertical momentum

1.1.9 Dirty Bomb and Transport Accidents

Both cases have in common that they are not predictable at all. Location and time of release can be known only after the event. Assessed values of the source term, of released thermal power or mass of the explosive device, and local weather data can be used to start an interactive dispersion calculation with RODOS. A time step length of 10 minutes is default. A special module is used to assess the rise and initial size of the cloud of a dirty bomb, and special parameters are used to assess the rise of the plume resulting from a transport accident with fire.

Transport Accident

For the calculation of plume rise in case of a transport accident with a fuel fire the same module is used as in case of a release from a NPP. But there is a different interpretation of input parameters: the venting area is changed into the burning area of the fuel, the exhaust velocity is set to zero, and the heat power of the fire has to be assessed.

Dirty Bomb

In case of an explosion of a dirty bomb, the initial height and position must be known. Furthermore assessed values of either the mass (TNT equivalent) or the explosive energy (= thermal energy of the explosion) of the device are needed to calculate the rise of the fireball and the radius of the cloud at the end of the rise. Here the formulas of HOTSPOT (described in [11]) are used:

$$m_{TNT} [kg] = E [MJ] / 4.6 \quad (\text{Eq. 12})$$

Rise Δh [m] of the fireball after explosion of m_{TNT} [kg] explosive; *corrfac* serves as a correction factor of the rise, if the user wants to modify it:

$$\Delta h = 70 \cdot m_{TNT}^{0.25} \cdot corrfac \quad \dots\dots\dots(\text{Eq. 13})$$

Radius of the cloud after rise [m]:

$$r_{cloud} = 17.5 \cdot m_{TNT}^{0.25} \quad (\text{Eq. 14})$$

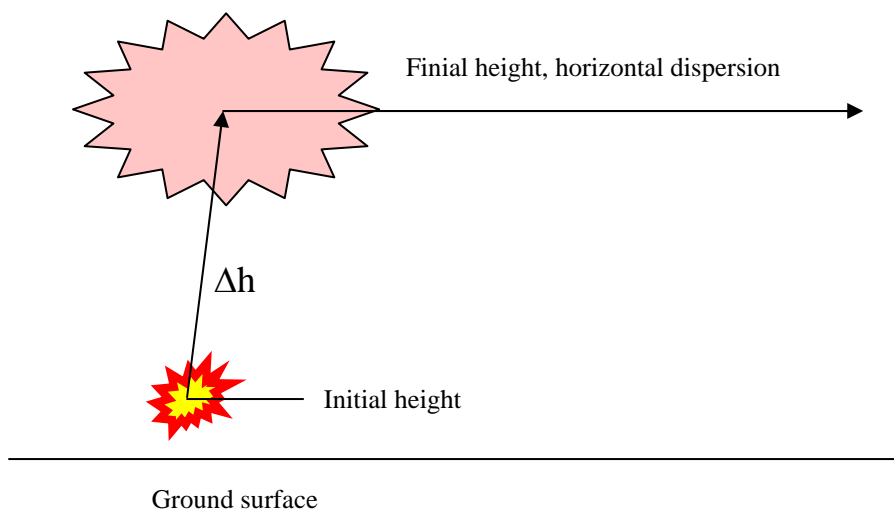


Fig. 7: Dirty Bomb Scheme

1.2 Deposition to surfaces and depletion of the cloud

In ATSTEP 4 groups of radioactive materials are distinguished according to their dry and wet deposition properties. These (deposition-) groups are:

- noble gases (neither dry nor wet deposition)
- elementary iodine, i.e. airborne I₂-vapor (dry and wet deposition)
- organically bound iodine, e.g. Methyl Iodide CH₃I (dry and wet deposition)
- aerosols, i.e. radionuclides in aerosol form or bound to aerosols, e.g. aerosol iodine, metal oxides (dry and wet deposition)

1.2.1 Dry deposition: deposition velocities

The contamination of a surface in contaminated air can be characterised by the deposition velocity v_d . It is defined as the ratio of the contamination rate dC_d/dt of the surface and the nuclide concentration in the ambient air χ :

$$v_d \left[\frac{m}{s} \right] = \frac{dC_d}{dt} \left[\frac{Bq}{m^2 s} \right] / \chi \left[\frac{Bq}{m^3} \right] = C_d / \int \chi dt = C_d / TIC \quad (\text{Eq. 15})$$

Correspondingly the ground contamination is calculated in ATSTEP during each time step from the time-integrated concentration in the air near ground and the deposition velocity. The deposition velocities of the deposition groups depend on the degree of vertical turbulent mixing of the air (atmospheric resistance) and on local surface properties (canopy resistance), which can be derived in a simplified manner from the land use. The deposition velocities are derived in this way in the Meteorological Preprocessor (MPP) using the DEPOSITION routines [6]. In the case of the interactive RODOS module QUICKPROGNO, as it works without the MP, the resistances and deposition velocities are calculated in the QUICKPROGNO-ATSTEP

The RODOS database contains land use information containing 5 classes:

- 1) Settlements, Urban or Industrial areas, 2) Pasture, 3) Agricultural areas, 4) Forest, 5) Water

Attention: The standard surface type used in RODOS and ATSTEP is lawn. In ATSTEP ground contaminations are calculated exclusively assuming this surface type. This holds also for the calculation of ground gamma radiation and local gamma dose rates, i.e., location factors =1 are assumed. This does not imply that the plume is depleted corresponding to the surface type lawn. For depletion calculations the land use pattern under each puff is considered. An effective depletion is derived for each puff during each time step from the local deposition velocities in the area of the puff (1.2.3).

Table 1 contains calculated example deposition velocities for the standard surface lawn in [m/s], with windspeed $u_{10} = 4$ [m/s]:

TABLE 1. Example deposition velocities in [m/s] for lawn[6], windspeed 4 m/s			
Surface type	elemental Iodine	organically b. Iodine	Aerosols
lawn	8.0 E-03	0.1 E-03	1.0 E-03

Depletion, dry

Due to mass conservation the material ΔQ taken from a puff during deposition corresponds to the surface contamination under the puff times the area ΔF covered:

$$\Delta Q[Bq] = -C_d \left[\frac{Bq}{m^2} \right] \cdot \Delta F[m^2] = -v_d \cdot TIC(x, y, 1m) \cdot \Delta x \Delta y \quad (\text{Eq. 16})$$

Integration of Eq. 16 gives the amount of material reduced by depletion of a vertically Gaussian puff during transport in x direction:

$$Q(x) = Q_0 \cdot \exp\left(-\sqrt{\frac{2}{\pi}} \cdot \frac{v_d}{u} \cdot \int_{x_0}^x \frac{1}{\sigma_z(x')} \cdot \exp\left(\frac{-h^2}{2\sigma_z(x')^2}\right) dx'\right) \quad (\text{Eq. 17})$$

The integral over the variable x' is solved numerically, as long σ_z is still growing and depends on x , i.e. if there is no homogeneous vertical mixing of the puff.

1.2.2 Wet deposition: Washout

Wet deposition is calculated using a washout model with the parameter $\Lambda[1/s]$. The contamination $C_w[Bq/m^2]$ is the product of the washout constant Λ , the precipitation duration Δt , and the integral of the vertical profile χ of the Gaussian puff:

$$C_w = \Lambda \cdot \Delta t \cdot \int \chi \cdot dz \quad (\text{Eq. 18})$$

The washout constant depends on the deposition group and the precipitation intensity I in $[mm / h]$:

$$\Lambda\left[\frac{1}{s}\right] = a \cdot \left(\frac{I}{1[mm/h]}\right)^b \quad (\text{Eq. 19})$$

In table 2 the values of a and b for different deposition groups are given:

TABLE 2. Parameters a and b for wet deposition [7]

deposition group	a	b
noble gases	0	0
aerosols	8.0 E-5	0.8
elementary iodine	8.0 E-5	0.6
org. bound iodine	8.0 E-7	0.6

Depletion, wet

The amount of material still in the puff after being washed out during the time t (or during transport in x direction with velocity u) is:

$$Q(x) = Q_0 \cdot \exp(-\Lambda \cdot t) = Q_0 \cdot \exp\left(-\Lambda \cdot \frac{x}{u}\right) \quad (\text{Eq. 20})$$

It is assumed that the cloud is washed out homogeneously over its full depth.

1.2.3 Deposition depending on location and puff depletion

Generally deposition processes depend on local conditions. Local land use defines the kind of surfaces (agricultural use, canopy, etc.) and by this influences the dry deposition velocities (surface resistance). Additionally the local state of turbulence of the atmosphere influences the resistance against vertical transport (atmospheric resistance). In the case of wet deposition the local precipitation intensity a local value of the washout parameter Λ . The local values of the deposition parameters v_D and Λ are defined as fields on the calculation grid, so that each grid cell has its own set of deposition parameters. Because the state of turbulence and precipitation can change this set is time dependent.

The concentration of the material staying in the depleted cloud after deposition is calculated assuming „source depletion“, i.e., the amount of material deposited from a puff onto a surface is taken from the puff as a whole, not only from the near to the surface parts of the puff’s volume. Because a puff generally covers more than one grid cell with locally different deposition parameters during the advection step, but the puff can only be depleted as a whole, its depletion can only be calculated with effective, puff-averaged deposition parameters. The exact way to determine these effective parameters is to calculate the concentration weighted average of the v_D - and Λ -values in all the grid cells under the puff.

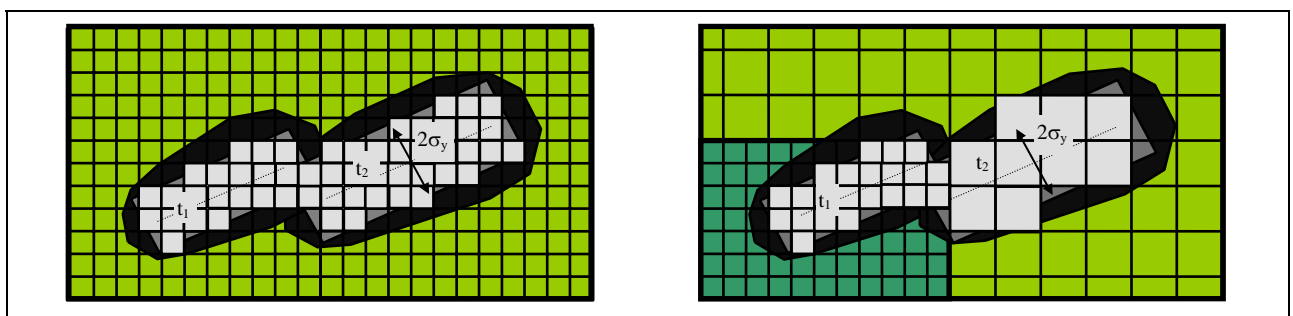


Fig. 8: Grid cells covered by the puff during time step t_1 to t_2 a) constant 41 x 41 cells grid, b) non-uniform grid

Instead of this in ATSTEP the simple average over the grid cells with the highest concentrations of the puff, i.e. the grid cells within the σ_y -surrounding of the puff axis, is calculated. For this purpose rectangles with $2\sigma_y$ width are constructed around the puff axes before and after the transport step (at times t_1 and t_2). Then the grid cells situated inside these rectangles are determined, and the averages of the deposition parameters in these cells are calculated. These averages are used as effective deposition parameters for determining the depletion of the puff in the step from t_1 to t_2 .

1.3 Radioactive decay and build-up of daughter nuclides

Radioactive decay is calculated at each time step for all nuclides during dispersion and deposition and is considered in the output fields concentration in air, ground contamination, potential doses and dose rates.

During atmospheric dispersion and deposition of radionuclides radiologically important daughter nuclides can be produced in the cloud and on contaminated surfaces. Resulting transformations of the chemical form of the nuclides and changes of their deposition properties can lead to complex contamination patterns. A general modelling and code simulation of the build-up, the transport, and the decay of daughter nuclides during the dispersion and deposition calculations is not carried out in ATSTEP. Computer storage and computation times needed for that would exceed the desired level by far. In order not to neglect striking or radiologically important radionuclides in spite of this, some special nuclide specific modellings concerning build-up, deposition, and decay of daughter nuclides are installed. In RODOS-ATSTEP version 4.0 (July 2000), RODOS 5.0 (2003), and RODOS 6.0 (2004) the mother-daughter pairs of nuclides **Te-132** and **I-132**, as well as **Kr-88** and **Rb-88** are taken into account.

Te-132 and I-132

If there is Te-132 in the calculated release the build-up of the daughter I-132 is considered. Because the Te-132 is released as an aerosol it is assumed that the daughter is an aerosol too and has the same deposition velocity. Dispersion, depletion, and deposition are the same for both nuclides so that the mother-daughter ratio in the air and on ground is only defined by radioactive build-up and decay. If there is I-132 already in the release, as a mixture of elementary, organically bound, and aerosol fractions, the mixing ratio is recalculated according to the additional quantity of the aerosol daughter iodine.

Kr-88 and Rb-88

If there is Kr-88 in the release the build-up of the daughter Rb-88 is considered. Kr-88 is a noble gas and does not deposit. Its daughter Rb-88 is assumed to be an aerosol and therefore deposits. In the Kr-Rb-88 cloud the mother-daughter ratio is defined by the radioactive build-up and decay, as well as by depletion of the daughter. The ground surface contamination with Rb-88 is locally produced by deposition from the Kr-Rb-88 cloud and decays again according to the temporal distance from that deposition. If there is Rb-88 already in the release it decays according to the temporal distance from the start of the release.

1.4 Gamma radiation fields

In ATSTEP nuclide specific and total gamma radiation fields are calculated. The fields are the gamma dose rates in [mSv/h] and doses in [mSv] from the contaminated air (cloud gamma radiation) and from the contaminated ground surface (ground gamma radiation). Furtheron the total local gamma dose rate (local dose rate) is calculated. All dose rates and doses are calculated at a height of 1m.

1.4.1 Cloud gamma radiation

The gamma radiation field of the cloud is the sum of the fields of each puff released. The puff fields are calculated separately during each time step of the dispersion calculation. Two methods of cloud gamma radiation calculation are used: the cloud gamma correction factor method and the gamma submersion method.

The cloud gamma correction factor method is usually (*) used at distances below 10 km. It was originally developed for saving computer time when calculating the plume gamma radiation for the straight line Gaussian plume model. In ATSTEP it is applied as a quick approximation for the long puff gamma radiation. A cloud gamma correction factor gives the ratio between the gamma radiation of a Gaussian plume concentration distribution and the radiation of a semi-infinite cloud with the same axis concentration. The correction factor is 1 for immersion in a homogeneous semi-infinite cloud. It is always < 1 for inhomogeneous Gaussian clouds, where the maximum concentration is on the axis. For the calculations in ATSTEP a pre-calculated matrix of cloud gamma correction factors for different types of sigma-parameters (differing in roughness length, plume height, and stability class) and for a grid of polar co-ordinates is used. The correction factor data are from Monte-Carlo gamma calculations [8]. Suitable interpolation allows the calculation of the nuclide specific cloud gamma dose rate at any location (x, y) relative to the plume:

$$\frac{d}{dt} D_{\gamma C}^{nuc}(x, y, 1m) \left[\frac{Sv}{s} \right] = DRF_C^{nuc} \left[\frac{Sv}{s} \cdot \frac{m^3}{Bq} \right] \cdot C_{axis}^{nuc}(x, y, h) \left[\frac{Bq}{m^3} \right] \cdot f_{corr}(x, y, h) \quad (\text{Eq. 21})$$

Here DRF_C is the nuclide specific cloud gamma dose rate factor for a semi-infinite cloud, $C_{axis}(x)$ is the plume axis concentration, and $f_{corr}(x,y,h)$ is the interpolated correction factor. The plume axis is directed along the x-co-ordinate axis at the height h. In ATSTEP instead of a plume gamma field the gamma field of long puffs have to be calculated. For this purpose the long puffs are interpreted as a plume segments with rounded ends (see Fig. 2). The corresponding gamma field is approximated by multiplying the plume axis concentration $C_{axis}(x)$ in Eq.21 with the error function difference $F(x)$ from Eq.3, now using an additional $\sigma_x=100m$ for the average range of gamma radiation in air.

The immersion method is usually (*) used at distances beyond 10 km when there is complete vertical mixing. It is assumed that the puff cloud gamma radiation is just proportional to the local air contamination $C_C(x,y,1m)$ in the puff and that the radiation is given by the semi-infinite cloud approximation:

$$\frac{d}{dt} D_{\gamma C}^{nuc}(x, y, 1m) \left[\frac{Sv}{s} \right] = DRF_C^{nuc} \left[\frac{Sv}{s} \cdot \frac{m^3}{Bq} \right] \cdot C_C^{nuc}(x, y, 1m) \left[\frac{Bq}{m^3} \right] \cdot F(x) \quad (\text{Eq. 22})$$

*) Under stable atmospheric conditions and elevated releases the distance of vertical mixing may be much larger than 10 km. Therefore the correction factor matrix was extrapolated in the radius dimension for use up to 40 km. The limiting radii depend on release height h and on PG-stability and are listed below:

Ranges RGAMFK of Correction Factor Application in Meter: 1,2,3,4,5,6 means the PG-Stability Class

h.GE. 10 m	h.GE. 75 m	h.GE.140 m	h.GE.200 m
RGAMFK(1)= 10000.	RGAMFK(1)= 10000.	RGAMFK(1)= 15000.	RGAMFK(1)= 15000.
RGAMFK(2)= 10000.	RGAMFK(2)= 10000.	RGAMFK(2)= 15000.	RGAMFK(2)= 15000.
RGAMFK(3)= 10000.	RGAMFK(3)= 10000.	RGAMFK(3)= 20000.	RGAMFK(3)= 20000.
RGAMFK(4)= 10000.	RGAMFK(4)= 10000.	RGAMFK(4)= 20000.	RGAMFK(4)= 20000.
RGAMFK(5)= 10000.	RGAMFK(5)= 10000.	RGAMFK(5)= 30000.	RGAMFK(5)= 40000.
RGAMFK(6)= 30000.	RGAMFK(6)= 30000.	RGAMFK(6)= 30000.	RGAMFK(6)= 40000.

1.4.2 Ground gamma radiation

The gamma radiation from the ground is proportional to the nuclide contamination C_G of the ground surface layer and is calculated by dose and dose rate conversion factors DRF_G for ground gamma radiation. The nuclide specific gamma dose rate is:

$$\frac{d}{dt} D_{\gamma G}^{nuc}(x, y, 1m) \left[\frac{Sv}{s} \right] = DRF_G^{nuc} \left[\frac{Sv}{s} \cdot \frac{m^2}{Bq} \right] \cdot C_G^{nuc}(x, y) \left[\frac{Bq}{m^2} \right] \quad (\text{Eq. 23})$$

A simplifying assumption is that the local gamma radiation comes from an infinite plane which has the local contamination everywhere. This approximation is not valid in the case of high gradients of the contamination over distances below 100 m. The vertical distribution of the contamination is not considered in the case of deposition to canopies (e.g. forest). Independent of local land use deposition to lawn is assumed everywhere and according to this the ground gamma radiation is calculated.

2 The ATSTEP-Code

The ATSTEP code (programming language: FORTRAN) is integrated in RODOS as a subroutine of the interactive prognosis modules **ALSMCprogn** and **QUICKPROGNO**, and the automatic diagnosis-module **Atstepdiagn** in the subsystem ASY. ATSTEP is called in each time step of a loop of the RODOS modules corresponding to the time steps of a dispersion prognosis or diagnosis calculation. The prognosis time step length may be 10 minutes but typically is 30 or 60 minutes, the diagnosis time step length is always 10 minutes.

2.1 ATSTEP in different RODOS ASY modules

2.1.1 ATSTEP in the prognosis module ALSMCprogn

During each 30 minutes time step **ATSTEP** is provided with data arrays of wind, stability, dry deposition resistance, and precipitation by the **Meteorological Preprocessor (MPP)**. The primary meteorological data that are processed for near range dispersion calculations in the **MPP** can come from different sources:

- prognostical weather data from national numerical weather prediction, in Germany DWD-data, in other countries ALADIN- or HIRLAM-data
- user selected weather data files or weather data from hand input

2.1.2 ATSTEP in the interactive module QUICKPROGNO

If the user wants to perform **quick interactive scenario calculations** with artificial weather data then the system can be run **without the MPP**. The weather data are put in by the user directly or in the form of selected weather data files. The programme system for this purpose is **QUICKPROGNO**.

2.1.3 ATSTEP in the diagnosis module Atstepdiagn

During an accident of a nuclear power plant with a radioactive release to the atmosphere the **Automatic Mode** of the RODOS system is running. This mode allows for a **real-time diagnosis** of the radiological situation with a cycle time of 10 minutes. During each 10 minutes time step **ATSTEP** is provided with the data arrays of wind, stability, dry deposition resistances, and precipitation by the **MPP**, and with nuclide specific release data from the source term processed by **STerm** [9]. The primary meteorological data, release-, and monitoring data come from the RODOS real-time data base, where the on-line measured data of the meteorological instrumentation and the stack instrumentation of the nuclear power plant and other measuring stations are sampled.

Direct continuation of the Diagnosis dispersion calculation in the Auto-Prognosis

There is a direct coupling of the diagnosis to the automatic prognosis calculation: the current positions, the instantaneous and time-integrated fields, and the activity contents of the puffs and all doses are transferred to the subsequent auto prognosis run. In this way the radiological situation that has developed in the past diagnosis can be smoothly continued by the prognosis.

2.2 Inner structure of the ATSTEP code

The inner loop structure of ATSTEP, the sequence and contents of subtasks is shown in the diagram in Fig. 8.

The initialisation is carried out during the first time step, at $M=1$. All concentration and dose arrays are set to zero, other variables get their initial values. During all later time steps with $M > 1$ this part is skipped.

The outermost DO-loop is the **loop over the released puffs**. These puffs have been emitted from the source from the start of the release at time step $M=1$ until the time step M (inclusively). In the prognosis mode the number of the puffs released is equal to M or less, because, if there are intervals with no releases, the corresponding puffs are omitted and not counted. In the diagnosis mode the number of released puffs is equal to the number of time steps as long as no puff has left the calculation area. In the puff loop the trajectories and the puffs' geometrical properties like location, orientation, and size are calculated. This includes the calculation of the height of the puff in the case of thermal rise and its local dispersion parameters (σ). Furthermore for mass balance each puff's remaining relative source term contents, which decreases due to depletion is calculated. This is carried out for each of the 4 deposition groups (noble gases, elementary iodine, organically bound iodine, and aerosols).

In order to avoid an unlimited increase of the number of puffs to be processed during a long run in the diagnosis mode, the puffs having left the calculation grid during time step M are discarded in the time step $M+1$. The remaining puffs are renumbered, and correspondingly all arrays with puff-related indices have to be rearranged (Subroutine **ATDIARENUM**). The time-integrated fields of the discarded puffs have to be saved and are stored separately.

The next DO-loop (nested in the puff loop) is the **loop over all relevant grid cell locations and detector positions** on the calculation grid. It serves to calculate each puff's normalised concentration, contamination, and radiation distributions at time step M and map them to the grid cell centres and the detector positions. Zero concentration calculations are avoided by defining frames for calculation dynamically around each puff. In these frames the Gaussian formulae, the error functions, the dispersion parameters, the time-integrations, and the cloud gamma radiation fields are calculated.

The next DO-loop (nested in the locations loop) is the **loop over the deposition groups**. Here the deposition and depletion, and the resulting concentration and radiation fields of the noble gases, elementary and organically bound iodines, and aerosols are calculated within the calculation frame of each puff.

The innermost DO-loop (nested in the deposition groups DO-loop) is the **loop over the nuclides** selected. Here the nuclide specific concentration and radiation fields are calculated by connecting the nuclide and time step specific source term and release information with the corresponding normalised fields of the puffs and deposition groups. The final fields are the sums over all contributing puffs with corrections for radioactive decay and partially build-up. They are calculated

at the end of each time step and are the basic output of the RODOS near range atmospheric dispersion modules for all grid cell and detector locations, and all nuclides:

ADIFMO: concentration in air near ground, instantaneous, [Bq/m³]
ADIFSU, DET0SU: concentration in air near ground, time step averaged, [Bq/m³]
ACH1SU: time-integrated concentration in air near ground, [Bq.s/m³]
ACH2SU: contamination of lawn, dry + wet, [Bq/m²]
ACH2WU, DET2WU: contamination of lawn, wet, [Bq/m²]
ACH3MO: cloud gamma rate dispersion factor, instantaneous, [Bq/m³]
ACH3SU: cloud gamma rate dispersion factor, time step averaged, [Bq/m³]
ACH400: cloud gamma dispersion factor, time-integrated, [Bq.s/m³]
IODFRAC: iodine fractions, instantaneous
REFELD, DETRER : precipitation rate [mm/h]

After this output **the DO-loops over the nuclides, the deposition groups, and the locations are finished.** In the prognosis mode now those puffs are transferred to input files for **the long-range dispersion module**, that have left the calculation grid of the near-range module (typically at 80 km source distance). **Then also the puff loop is finished.**

The programme is ready for calculating the next time step in the M+1. cycle of a prognosis or diagnosis calculation. At the beginning of the M+1. time step ATSTEP needs a part of the local variables to have the values of the preceding time step M. In the prognosis mode this is done using the option „**save locals on**“, so the locals are saved and not set to zero automatically on subroutine call.

In the diagnosis mode this is not possible because the execution of the diagnosis module is finished after each calculation step and memory is closed down. Therefore a **stop and restart mechanism** is used: At the end of each diagnosis time step all geometrical information containing position and orientation of trajectories and puffs, and all time integrated fields are stored in files (Subroutine **ATDIASTORE**). At the beginning of each new diagnosis time step these files are read in again (Subroutine **ATDIAREAD**). In this way the diagnosis can be continued without forgetting the past.

2.3 Subsequent programmes of ATSTEP

Within each prognosis- or diagnosis- time step cycle the dispersion and deposition calculation is followed by further programmes describing the current radiological situation. The programmes **ADORAT** and **ADOPOT** serve for calculation of current dose rates and potential doses and are used in the prognosis mode as well as in the diagnosis mode. The programmes **TIMEIN** and **DOSBAU** are used only in the prognosis mode, on the one hand to calculate cloud arrival times and on the other hand to produce dose bricks for a possible subsequent **EmerSim** [10] run (early countermeasures simulation).

ADORAT calculates dose rates from external gamma radiation and the nuclide specific cloud gamma dose at time step M. In detail the output consists of the following arrays on the calculation grid:

ACH3MO:	nuclide specific cloud gamma dose rate, instantaneous, [mSv/h]
ACH3SU:	nuclide specific cloud gamma dose rate, time step averaged, [mSv/h]
ACH4SU:	nuclide specific cloud gamma dose, [mSv]
DRNUGR:	nuclide specific ground gamma dose rate, [mSv/h]
DOSRCL:	cloud gamma dose rate, instantaneous, [mSv/h]
DOSRGR:	ground gamma dose rate, [mSv/h]
ODLDOS:	local gamma dose rate, [mSv/h].

The following data output comes for detector locations:

DETRCL:	cloud gamma dose rate, instantaneous, [mSv/h]
DETODL:	local gamma dose rate, [mSv/h].

ADOPOT calculates current potential organ doses from external gamma radiation, from inhalation, and the local skin dose up to time step M. In the case of external gamma radiation a "current" dose means the dose received up to the current simulation time step. In the case of inhalation it means the committed (50 years) inhalation dose, that results from an inhalation up to the current time step. In the case of the local skin dose it means the dose, that is absorbed in the skin and caused by a contamination, deposited up to the current time step. In detail the output consists of the following arrays on the calculation grid:

DOSPCL:	current pot., organ specific cloud gamma dose, [mSv]
DOSPGR:	current pot., organ specific ground gamma dose, [mSv]
DOSPIH:	current pot., organ specific inhalation dose (committed), [mSv]
DOSPSL:	pot., local skin dose from current skin contamination, [mSv]

TIMEIN calculates the array of cloud arrival times on the calculation grid. The arrival of the cloud at a location can be defined by the number of accumulated radioactive decays per cubic metre in the

air near ground, i.e. the time-integrated activity concentration ACH1SU summed over all nuclides [Bq.s/m³]. If this number exceeds the value 1000 [Bq.s/m³] in the M-th time step, the local arrival time of the cloud is set to the value M/2 [h]. The following array is output on the calculation grid:

- TIMFEL:** cloud arrival times at the locations on the calculation grid, [h]
- DOSBAU:** At the end of the prognosis time interval on the last day of the scenario DOSBAU generates potential dose bricks for the dose calculations with early emergency actions in **EmerSim**. In the case of external gamma radiation the dose brick of a specified exposure pathway and organ is defined as the amount of dose absorbed in the M-th half hour time step. In the case of inhalation or skin contamination it is defined as the amount of dose resulting from inhalation or deposition during that time step. The following arrays on the calculation grid are put out for 5 organs after each of the maximum 48 time steps of the last day of a prognosis calculation:
- DBAUCL:** organ specific dose brick for cloud gamma radiation, [Sv]
- DBAUGR:** organ specific dose brick for ground gamma radiation, [Sv], exposure time = 0.5 h
- DINTGR:** organ specific dose brick for ground gamma radiation, [Sv], for longer exposure with times = 1d, 7d, 14d, 30d, 0.5y, 1y, 50y
- DBAUIH:** organ specific dose brick for inhalation, [Sv], integration times = 1d, 7d, 30d, 1y, 50y
- DBAUJT:** thyroid dose brick for iodine inhalation, [Sv], integration times = 50y
- DBAUSL:** dose brick for local skin dose by contamination, [Sv]
- DBAUSLW:** dose brick for local skin dose by wet contamination, [Sv]
- DBAUSO:** organ specific dose brick for gamma radiation from contaminated skin and clothes, [Sv]
- DBAUSOW:** organ specific dose brick for gamma radiation from wet contaminated skin, and clothes, [Sv]

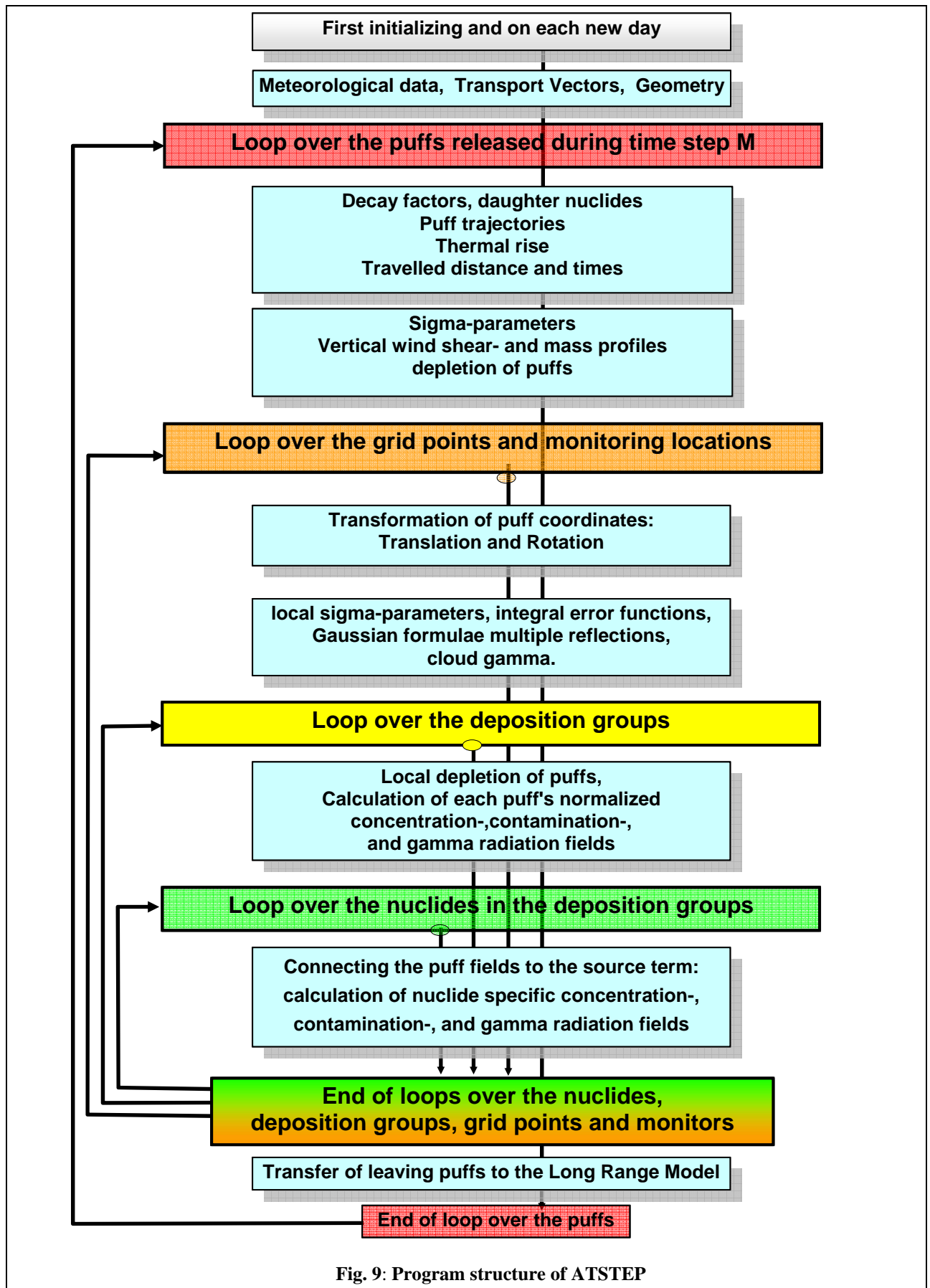


Fig. 9: Program structure of ATSTEP

3 References

- [1] Panitz, H-J., Matzerath, C., Päsler-Sauer, J., *UFOMOD, Atmospheric Dispersion and Deposition*, Report KfK-4332, (1989)
- [2] Störfall-Leitlinien, Bundesanzeiger, Jahrg. 35, Nummer 245a, 1983, Der Bundesminister der Justiz.
- [3] German French Commission, *Das deutsch-französische Modell für die atmosphärische Ausbreitung in Unfallsituationen*, DFK-Bericht 92/2, AG3, 06.1992, Dresden.
- [4] Hanna, S. R., Briggs, G. A., Hosker, R. P., *Handbook on Atmospheric Dispersion*, U. S. Department of Energy, 1982, DOE/TIC-11223, S. 31
- [5] Briggs, G. A., *Plume Rise Predictions*, in *Lectures on Air Pollution and Environmental Impact Analyses*, Workshop Proceedings, Boston, Mass., 1975, AMS, Boston, Mass.
- [6] Müller, H., Gering, F., *Documentation of the Deposition Module in RODOS PV5.0*, Technical Note RODOS(RA3)-TN(02)01.
- [7] Schwarz, G., *Deposition and Post-Deposition Radionuclide Behaviour in Urban Environments*, Proceed. of Workshop on Methods for Assessing the off-site Radiological Consequences of Nuclear Accidents, 15-19 April 1985, Luxembourg, Commission of the European Communities, Report EUR 10397 EN, 1986, p. 542
- [8] Jacob, P., Müller, H.M., *Gamma Exposure from Bi-Gaussian Clouds*, GSF.
- [9] Landman, C., *Code Package STerm in RODOS PV 5.0*, RODOS technical note, RODOS(RA1) TN(02)-01
- [10] Päsler-Sauer, J., *Model Description of the Early Countermeasures Module EmerSim in RODOS PV 6.0*, RODOS technical note, RODOS(RA3) TN(04)-03
- [11] Deaves, D.M., Hebden, C.R., *Aspects of Dispersion following an Explosive Release*, Atkins Process, Document of the UK Atmospheric Dispersion Modelling Liaison Committee

Document History

Document Title:	Description of the Atmospheric Dispersion Model ATSTEP Version RODOS PV 6.0 Final
RODOS number:	RODOS(RA2)-TN(04)-03)
Version and status:	Version 2.0 (draft)
Authors/Editors:	Jürgen Päsler-Sauer
	Address:
	Forschungszentrum Karlsruhe GmbH
	Institut für Kern- und Energietechnik
	Postfach 3640
	D-76021 Karlsruhe
Issued by:	FZK RODOS Team
History:	none
Date of Issue:	June 2004
Circulation:	all
File Name:	ATSTEP2007.doc
Date of print:	July 30, 2007